THE ASTROPHYSICAL JOURNAL, 544:550–557, 2000 November 20

MICROSCALE STRUCTURES ON THE QUIET SUN AND CORONAL HEATING

V. ALETTI,[1] M. VELLI,[2,3] K. BOCCHIALINI,[1] G. EINAUDI,[3,4] M. GEORGOULIS,[5] AND J.-C. VIAL[1]

Received 1999 October 6; accepted 2000 July 6

ABSTRACT

We present some results concerning transient brightenings on the quiet Sun, based on data from the Extreme-Ultraviolet Imaging Telescope on board the *Solar and Heliospheric Observatory*. Histograms of intensity are found to be well fitted by χ^2 distributions for small values of the intensity, while at high intensities power-law distributions are always observed. Also, the emission presents the same statistical properties when the resolution is downgraded by local averaging; i.e., it appears to be self-similar down to the resolution scale of the instruments. These properties are characteristic of the emission from a forced turbulent system whose dissipation scale is much smaller than the pixel dimension. On the basis of the data presented as well as other published results and our present theoretical understanding of MHD turbulence, we discuss the realism of the nanoflare scenario of coronal heating.

Subject headings: MHD — Sun: corona — Sun: flares — turbulence

On-line material: color figures

1. INTRODUCTION

Recently, the idea that coronal heating may be described in terms of MHD turbulence has gained much ground. At the same time, experimental investigations of solar emission aimed at ascertaining the feasibility of the nanoflare scenario of coronal heating are being carried out at an accelerating pace.

Solar flares prove that at least at large energies (10^{28}–10^{32} ergs) coronal dissipation occurs in bursts, lasting anywhere from a few minutes up to hours, with the main part of the energy going into the acceleration of electron particle beams (Crosby, Aschwanden, & Dennis 1993), ion beams (Ramaty et al. 1995), and the X-ray emission of the thermal plasma (Wu et al. 1986). The power-law distribution of the number of flares as a function of total estimated energy content (down to energies of order 10^{27} ergs) led Lin et al. (1984) to suggest that in fact all of coronal heating could be accounted for by smaller flarelike events labeled "microflares."

In order for nanoflares-microflares to provide sufficient energy for heating the corona, the low-energy distribution of events as a function of energy must depart from that observed at higher energies (Hudson 1991). This is because the total energy is dominated by low-energy or high-energy events depending on whether the power-law index α is less than or greater than -2 and because high-energy events are clearly not sufficient to account for the heating; the dissipated flux for a large flare is 10^7 ergs cm^{-2} s^{-1}; i.e., it is comparable to global heating losses, but the corona exists all the time, while large flares occur only occasionally. For nanoflares to be a viable heating mechanism, it is therefore necessary for the power-law index to decrease with decreasing energy from its large energy value $\alpha \simeq -1.6$, -1.8 below $\alpha = -2$. An attempt at determining the behavior of coronal emission at extremely low energies, outside of active regions, has been made recently by Krucker & Benz (1998, hereafter KB), using the variations of emission measure in Fe lines images of the quiet Sun obtained by the Extreme-Ultraviolet Imaging Telescope (EIT) on the *Solar and Heliospheric Observatory SOHO*. From their images, taken in rapid succession over a period of about 40 minutes, KB identify a number of "events" by looking for peaks in the emission measure in a given pixel and following them in time. With some hypotheses concerning filling factors and energetics, KB then determine the overall energies (in the range 10^{25}–10^{26} ergs) and histograms thereof, obtaining a power law with spectral index $\alpha \simeq -2.6$. They interpret this as evidence in favor of nanoflare heating for the solar corona. Berghmans, Clette, & Moses (1998) also analyzed EIT images, showing that the Fourier transforms of intensities obey power laws with various spectral indices. In their case histograms of He II and Fe XII "events" display power-law indices of -1.8 and -1.35, respectively. This discrepancy may be only apparent, but what is real is the problem of defining an "event" and, above all, of deriving from the data the energy associated to it. Let us describe some of the uncertainties involved with such modeling in more detail.

From a closely spaced temporal sequence of images, KB identify a number of brightenings using an algorithm to distinguish between two different events occurring in nearby pixels from larger events covering many pixels. They then proceed to estimate the energy input as that required to bring the plasma up to the given density and temperature so that

$$E_{\rm KB} = 3k_B T\sqrt{\Delta M A q h}\,,$$

where ΔM is the variation in emission measure, q is a filling factor, A the areal extent of an "event," and h the height. In this equation, A and ΔM are determined from observations, while the filling factor and event height, or rather the product Aqh, is assumed constant. Berghmans et al. (1998), on the other hand, consider the radiative energy loss associated with the observed line in an event, estimated as the integrated emission measure over the duration multiplied by the radiative-loss function calculated at the correspond-

[1] Institut d'Astrophysique Spatiale, Bâtiment 121, Université Paris XI-CNRS, F-91405 Orsay Cedex, France.

[2] Dipartimento di Astronomia e Scienza dello Spazio, Università di Firenze, Largo Enrico Fermi, 5, 50125 Firenze, Italy.

[3] Istituto Nazionale Fisica della Materia, Sez. A, Università di Pisa, 56100, Pisa, Italy.

[4] Dipartimento di Fisica, Università di Pisa, 56100 Pisa, Italy.

[5] Department of Physics, University of Thessaloniki, GR-54006 Thessaloniki, Greece.

ing temperature. Assuming that the event-counting algorithms used are compatible, there is a straightforward relation that should be satisfied by the two power laws. In essence, KB report histograms of the integrated emission measure $\Delta M^{1/2}$, while Berghmans et al. (1998) report histograms of ΔM. Hence, from a scaling point of view, we may say that the two energies are related by $E_{\rm KB} = E_{\rm B}^{1/2}$. Now had the two analyzed exactly the same data with the same counting algorithm, the total number of events would be the same and therefore $N(E_{\rm B})dE_{\rm B} = N(E_{\rm KB})dE_{\rm KB}$ or $N(E_{\rm B}) = N(E_{\rm KB})dE_{\rm KB}/dE_{\rm B}$. If α is the KB power-law index, $N(E_{\rm KB}) \sim E_{\rm KB}^{\alpha}$, and then we find $N(E_{\rm B}) \sim E_{\rm B}^{(\alpha-1)/2} \sim E_{\rm B}^{-1.8}$. Berghmans et al. find in this case an index of -1.35, a discrepancy, which may be due both to differences in the data sets and, more probably, to differences in the definition of individual events. KB assumed that Aqh did not depend on event energy. On the other hand, using the same argument, one may explore the effect a correlation between filling factor (and event height) and its emission measure would have on the distribution of event energy. Assuming a dependence $Aqh \sim E^{\beta}$ (where reasonably β should be positive and of order 1 or less) and as usual that the total number of events remains the same, one obtains $E_{\rm KB} \sim E^{(1-\beta/2)}$. The new distribution therefore becomes $N(E) \sim E^{\gamma}$, where $\gamma = \alpha(1-\beta/2) - \beta/2$, which, for a positive $0 < \beta < 1$ and $\alpha < -1$, yields $\gamma > \alpha$, i.e., a flattening of the spectrum compared to KB. Given such uncertainties, one should not place too much confidence in the value of the exponents. Here we focus on other aspects of emission properties that may provide more definite evidence concerning the nanoflare scenario.

In § 2 we will discuss some properties of MHD numerical simulations clarifying the small-scale physical mechanisms underlying the nanoflare scenario in order to place the data analysis into perspective. Then, in § 3, by using EIT data, we study the distribution of intensity of single pixels to check whether emission at coronal temperatures on the quiet Sun displays an excess of high-energy pixels and/or scale-invariance properties in the same way as in MHD turbulent systems. In § 4 we use the similarities between our findings and previous theoretical research to derive insights on the existence of microstructures that are the sites where current dissipation responsible for coronal heating occurs.

2. MHD-TURBULENCE SIMULATIONS AND THE NANOFLARE SCENARIO

In the nanoflare scenario, introduced by Parker (1988), dissipation occurs in individual current sheets arising from the dynamics of coronal magnetic field lines attempting to rearrange themselves into an equilibrium situation when subject to random footpoint shuffling. Imposing the value of the overall mean dissipation to be equal to the average coronal energy loss of 10^7 ergs cm^{-2} s^{-1} (Withbroe & Noyes 1977) and assuming a 100 G mean axial field, Parker (1988) found that the external forcing responsible for the energy input must produce a mean transverse component in the coronal field of approximately $B_{\perp}/B \simeq 0.25$ in a timescale of the order of 15 hr. Parker then imagined the buildup of such a field as occurring over substeps of the size and duration of a granule and associated a current sheet with each of these steps, reaching the conclusion that the energy liberated by the dissipation of the individual current sheet should be of the order of 10^{24} ergs.

Einaudi et al. (1996), Georgoulis, Velli, & Einaudi (1998), and Dmitruk, Gomez, & DeLuca (1998) interpreted the Parker scenario in terms of magnetically dominated MHD turbulence within a section of a coronal loop. In all sets of published simulations the average dissipation in the simulation box as a function of time was shown to be intermittent; i.e., the dissipation time series filtered at higher and higher frequency was shown to display an ever more bursty nature. An example is shown in Figure 1*a* where the original time series for the dissipation found by Georgoulis et al. (1998) is displayed and Figure 1*b* where the same series is shown subject to high-pass filtering. It is seen that the dissipation is more bursty at higher frequency, which is one definition of intermittency. An analogous situation also holds for the spatial distribution and is a universal feature of turbulence, where an approximate self-similarity in the inertial range (leading to the well-known Kolmogorov or Kraichnan energy distribution power laws with scale in the MHD case) gives way to strong intermittency in the dissipation range. This is observed provided there is a sufficiently wide inertial range, or separation of scales between the scales at which most energy is injected and those at which it is dissipated. In other words, a significant range of scales over which nonlin-

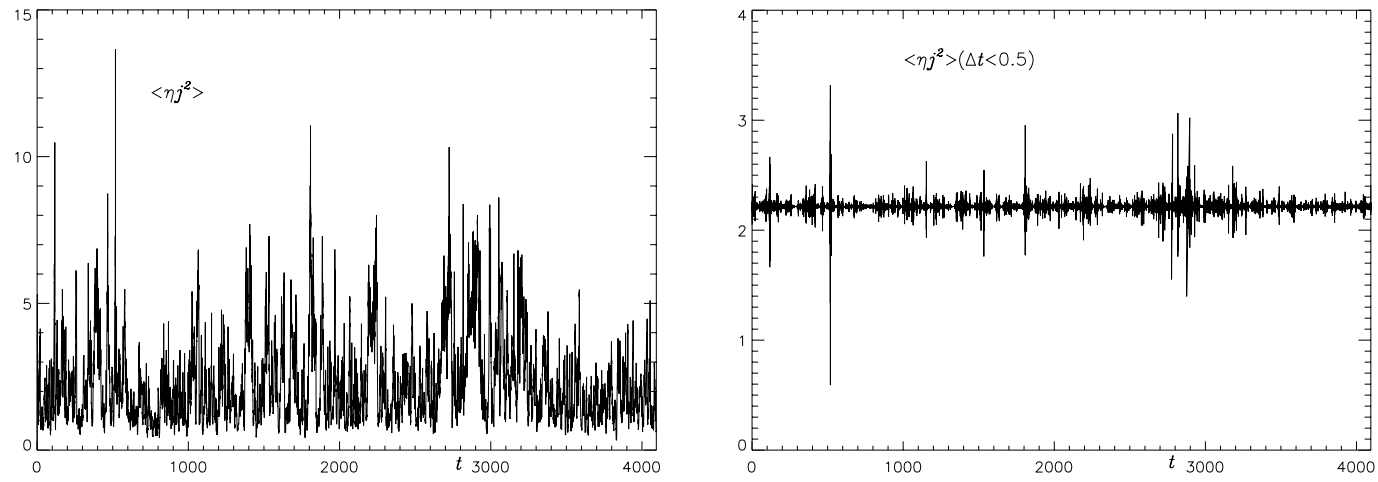

FIG. 1.—Time series of dissipation in a magnetically forced turbulence simulation from Georgoulis et al. (1998) (*left*). The same series subject to filtering of the low frequencies shows the intermittent nature of the signal (*right*).

ear dynamics occurs is the backdrop for the intermittent character of power dissipation.

One may attribute the properties of the statistics of the dissipation range to small-scale energy-release events. In the time series shown above one may define a simulation flaring event as any peak significantly above average. More properly, such events may be defined from histograms of dissipation intensity that show that for high intensity the distribution deviates from a Gaussian. Setting the level of noise at the intensity where such a departure occurs, one can define events every time the signal rises above noise. The resulting distribution of events displays a power law in energy, peak luminosity, and duration. To any single flaring event in the time series of average dissipation, there corresponds, within the simulation domain, a collection of many current sheets of varying intensity, so that the energy of individual "spatial" dissipative events is in fact much smaller than the total energy dissipated within the flaring event. Estimates of such energies have been deduced by Einaudi & Velli (1999); a random footpoint shuffling, due to photospheric velocities of the order of 1 km s^{-1}, induces in a magnetic structure of length $L = 10^4$ km and transverse dimension $l = 10^3$ km, with an axial magnetic field of 100 G and a density of 10^9 cm^{-3}, a turbulent state with an associated time-and-spaced–average dissipated flux of about 5×10^5 ergs cm^{-2} s^{-1}. The energy associated with individual "flaring" events ranges from 2×10^{23} to 2×10^{26} ergs. The transverse section chosen above, and the numbers used in the simulations, imply that the numerical simulation box corresponds to a single observational pixel. We therefore attempt an analogous data analysis on pixel images, carrying out a statistical analysis of the emission observed on the quiet Sun.

In § 3 we will show indeed that the high-intensity portion of the pixel-intensity distribution for a series of snapshots from quiet-Sun regions deviates significantly from the χ^2 (Gaussian) fit and that in such regions power laws are obtained that are practically insensitive to image resolution, just as would be expected if indeed the present observational resolution is much coarser than the dissipative scale on the Sun and nonlinear dynamics plays a fundamental role in the processes leading to the observed emission.

3. OBSERVATIONS

The quiet Sun has actually proved to be everything but quiet, the only difference with active regions being the reduced dimension of the areas of activity. An average quiet-Sun region appears to contain bright points, jets, or more generally knots of enhanced emission, with respect to the background average corona, of all spatial dimensions. We first concentrate on the statistical distribution of intensities of the single pixels (to be compared with the histograms of the spaced average dissipation in the numerical box) to derive a definition of "bright" pixels, and then we buildup statistics of spatial events.

3.1. *Global Statistical Analysis of the Whole Images*

We use a number of observations performed with *SOHO*, consisting of 21 full-Sun images taken between 1996 April 1 and 1997 April 13, in a line of Fe XII (195 Å), formed at 1.6×10^6 K with the EIT (Delaboudinière et al. 1995). We extract a part of these full-Sun images centered on the Sun center, 1 solar radius wide, in order to avoid active regions and to focus on the quiet Sun. Usual corrections are applied to all images (flat-fielding, grid subtraction, etc.), using standard EIT software. Because exposure times differ, corrected images are normalized and expressed in (arbitrary) EIT units; the spatial resolution is 2.″6, while the field of view of each image varies because images have been cropped to avoid active regions.

All images have been analyzed collectively in order to build intensity distributions that are statistically significant. We have selected images with at least a 5 day parsing to ensure that enough time for a complete restructuring of the small-scale magnetic field has elapsed (Schrijver, Title, & Van Ballejooijen 1997). In this way the same event is never counted twice, and statistical independence of the data set is ensured. Also, we have been careful to avoid images with a difference stronger than 10% in average intensity with respect to global average in order to avoid ambiguity in the definition of brightenings. The overall statistical sample is made up of a total of 5×10^6 pixels whose intensity histogram is shown on a log-log scale in Figure 2*a*. The distribution function is fitted with a χ^2 function in the central core of the distribution, which can therefore be interpreted as a noise. The fit departs from the data in two regions:

1. One at large intensity for intensities larger than a threshold I_B (Fig. 1). The distribution function is fitted by a straight line, with a slope equal to -4.87.
2. One at low intensity, which clearly belongs to a different distribution. This second deviation appears to be associated with darker regions in our images that, at least in one case, may be associated with the remnant of a polar coronal hole. Its presence may therefore be an indication of an underlying different magnetic topology (open vs. closed field lines) and probably a different dynamics and will not be discussed further in this paper.

The fact that the high-intensity portion of the distribution deviates significantly from the χ^2 (Gaussian) fit is a feature that has been found in many other *SOHO* data sets; in particular, Harrison (1997) identifies such tails in O IV with the presence of blinkers. On the other hand, such tails are found also in the distribution functions of the total dissipated energy obtained in forced MHD simulations (Georgoulis et al. 1998), as shown in § 2. We are tempted to interpret the data in the same way, i.e., as proof that (1) the dimensions of the single pixel (analogous to the numerical box) are large with respect to the dissipative scale, and (2) nonlinear dynamics play a fundamental role in the processes leading to the observed emission.

If this is true, we expect that this feature would be maintained when increasing the ratio between pixel dimension and dissipative scale, with some variation of the slope. We have checked whether this is the case in the data by decreasing the resolution of the original images by factors of 4 and 9, and the results are reported in Figures 2*b* and 2*c*, respectively. It is clear that the resulting intensity histograms retain the same features, with the high-intensity tails well fitted by power laws with similar spectral indices (Table 1). The small decrease of the index with decreasing resolution can be interpreted as a signature of intermittency, in the sense that looking at smaller and smaller scales one observes stronger and stronger departures from Gaussian statistics. It is then likely that similar intensity histograms

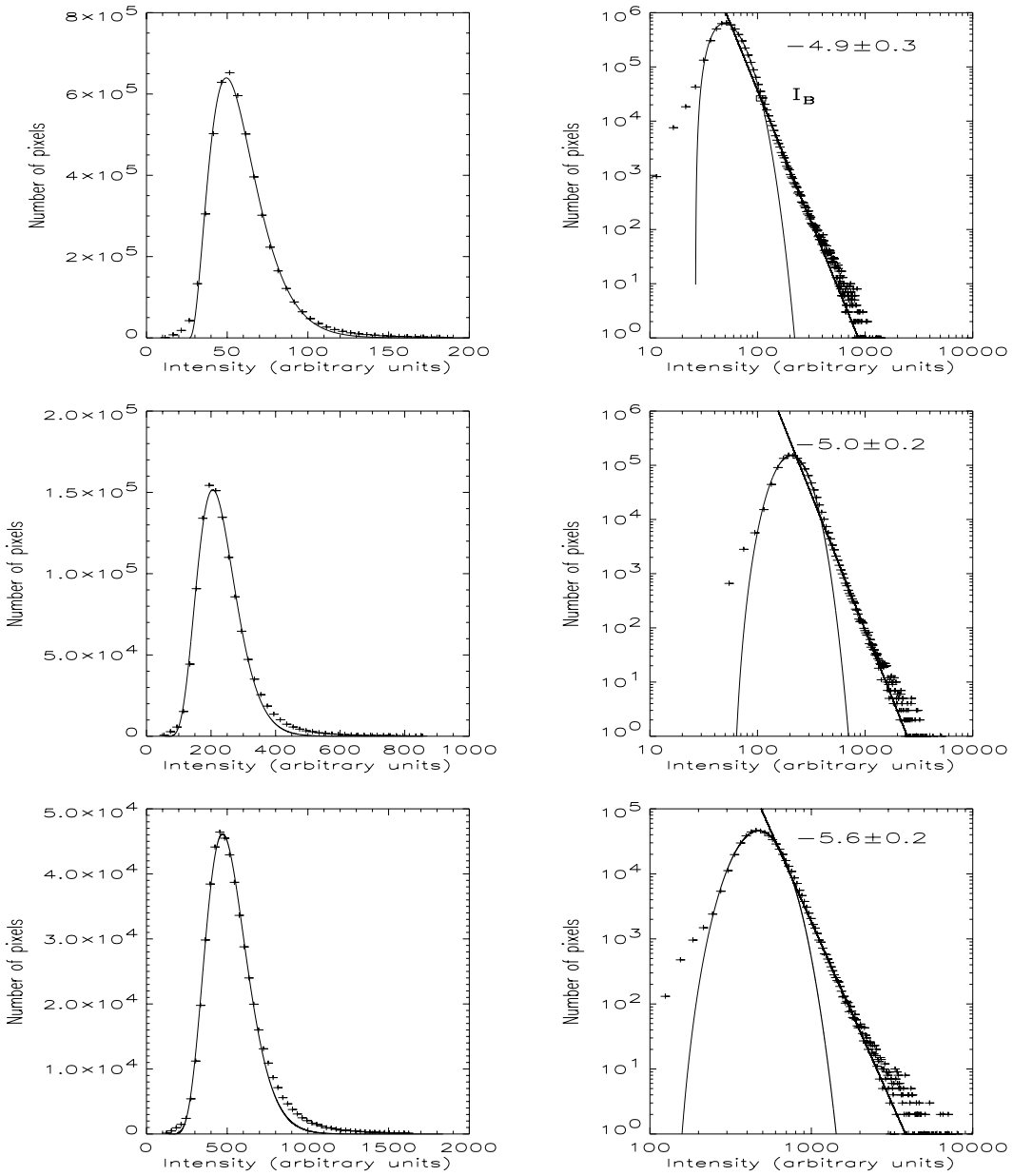

FIG. 2.—Pixel-intensity distribution of the original images (linear scale on the left, logarithmic scale on the right) (*top panel*), compared with distributions obtained decreasing the resolution by a factor of 4 (*middle panel*), and by a factor of 9 (*bottom panel*).

would be found at resolutions better than the observational one down to a scale close to the dissipation scale, which could be as small as the ion gyroradius (∼a few meters).

3.2. *Statistical Analysis of Isolated Bright Features*

The qualitative agreement between theory and observations described above supports the idea that the emission observed in one pixel is made up by emission from many subresolution sites and therefore that there should exist a statistical "elementary event" that can be seen as the building block of the activity in the regions examined. A brightening, which may cover from one to many pixels, is then built up from the coherent excitation of a large number of "elementary events"; the apparent spatial extent then depends on the correlation length of the magnetic structure involved. The quantitative definition of a brightening ("observed event") allows for some ambiguity. We have made the choice of defining an event as the collection of neighboring "bright" pixels, where we have used two different criteria to define the brightness based on the standard deviation σ deduced from the single-pixel histograms (§ 3.1). The first criterion (1) uses a definition of bright pixels as those whose intensities are larger than 2 σ and the second (2) larger than 3 σ above average, respectively. We notice that criterion 1 is equivalent to defining as "bright" all pixels whose intensity is above the threshold I_B.

TABLE 1

TOTAL INTENSITY DISTRIBUTION POWER-LAW INDICES

Parameter	Original Image	Binned by a Factor of 4	Binned by a Factor of 9
Power-law index.....	−4.9	−5.0	−5.6
Error bars.....	±0.3	±0.2	±0.2

NOTE.—Determined with different spatial resolutions on the same temporal sequence of EIT images.

An "observational event" is then energetically defined as the summation of the intensities of all neighboring "bright" pixels, and its size is defined as the overall dimension of the collection of such pixels. We obtain 4452 events using the criterion 1, with a total of 134,615 "bright" pixels and 2467 events (56,911 total pixels) adopting the second one. Figures 3 and 4 show the histograms of such events as function of their intensities (*left panel*) and dimensions (*right panel*) for the two cases examined, respectively. The histograms have been built using a variable bin size that increases by an order of magnitude every time the intensity (dimension) changes by an order of magnitude. The intensity histograms demonstrate that the selection process (i.e., the 2 σ vs. 3 σ choice) does not influence the resulting distributions, which

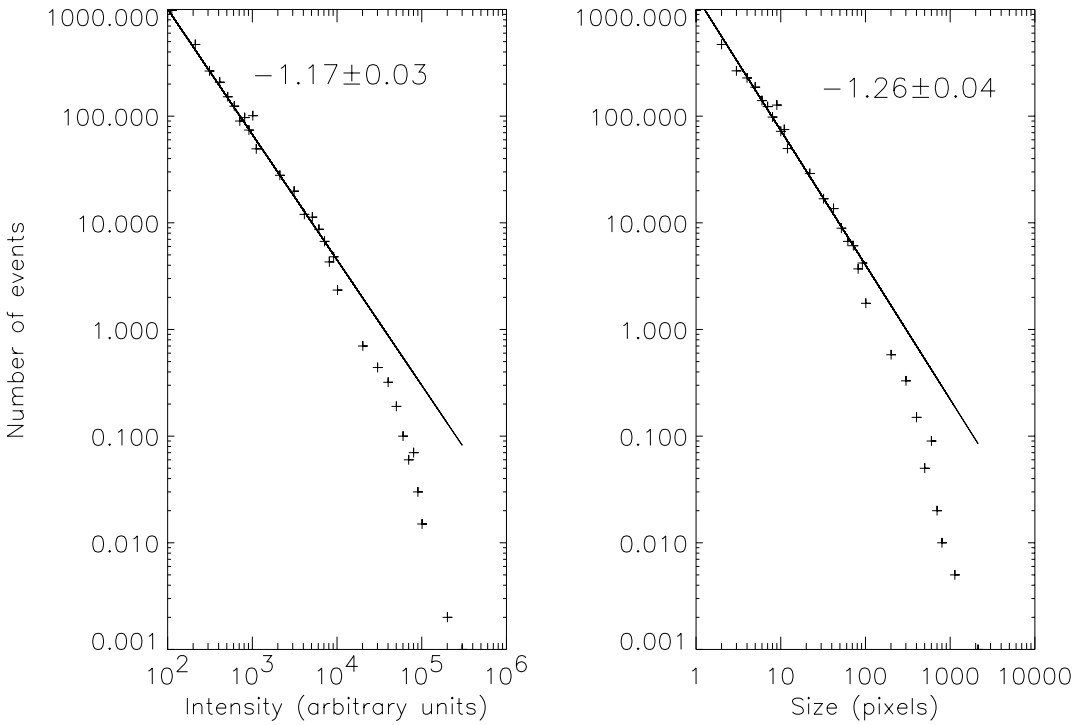

FIG. 3.—Histograms of intensity (*left panel*) and dimension (*right panel*) with 2 σ

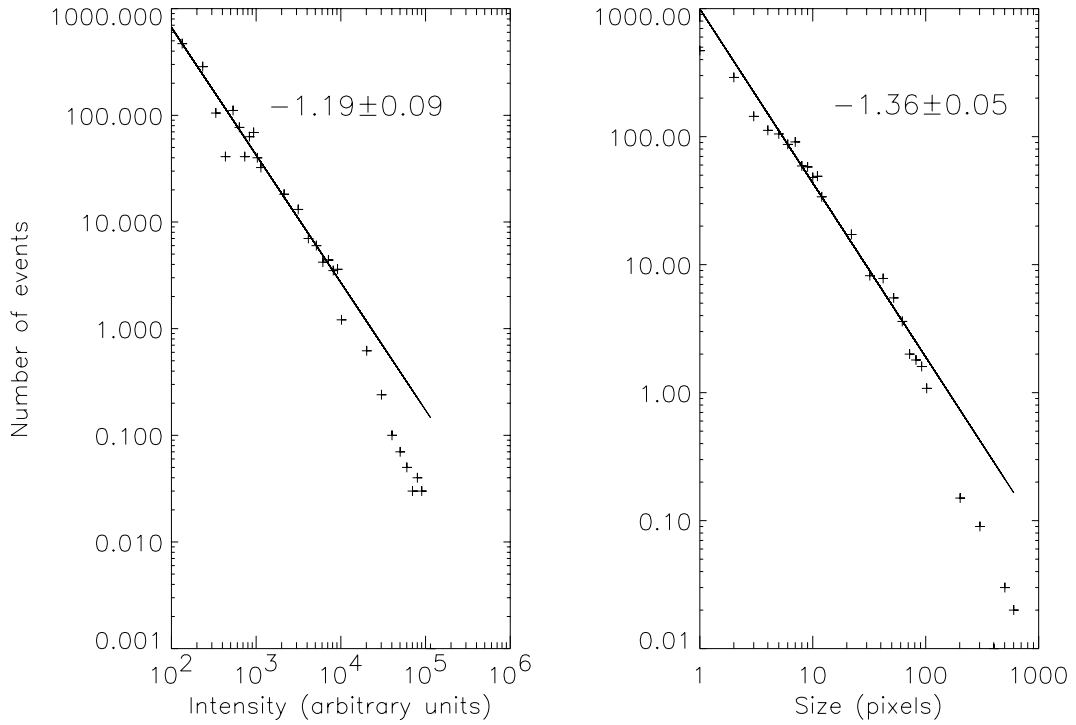

FIG. 4.—Histograms of intensity (*left panel*) and dimension (*right panel*) with 3 σ

TABLE 2

HISTOGRAM POWER-LAW INDICES

Histogram	2 σ	3 σ
Intensity.....	-1.17 ± 0.03	-1.19 ± 0.09
Size	-1.26 ± 0.04	-1.36 ± 0.05

NOTE.—Determined for the two kinds of histograms (intensity and size) and for the two different criteria.

appear to be described by the same power-law index within error bars (see Table 2). The similarity in the dimension and intensity distributions implies that different total event intensities essentially are due to their differing dimensions rather than to significant single pixel-intensity variations. This means that the basal intensity is approximately the same for all events.

It is interesting to show how the images appear after retaining only such events. In Figure 5 we give an example

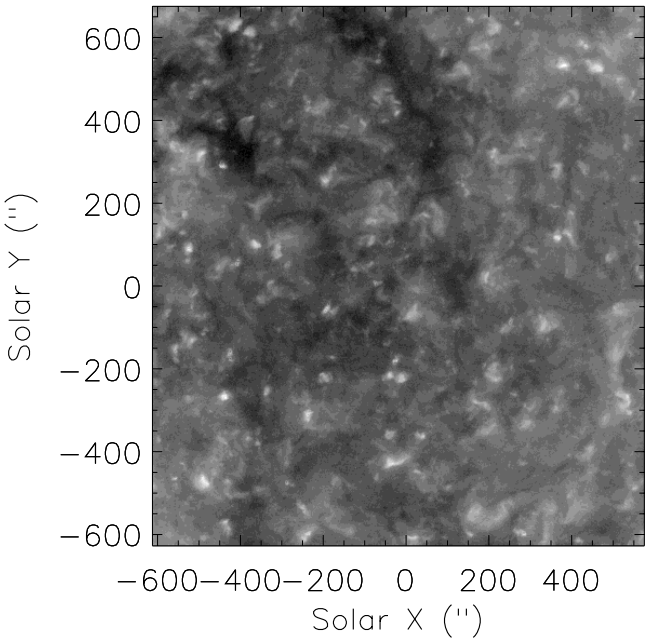

FIG. 5*a*

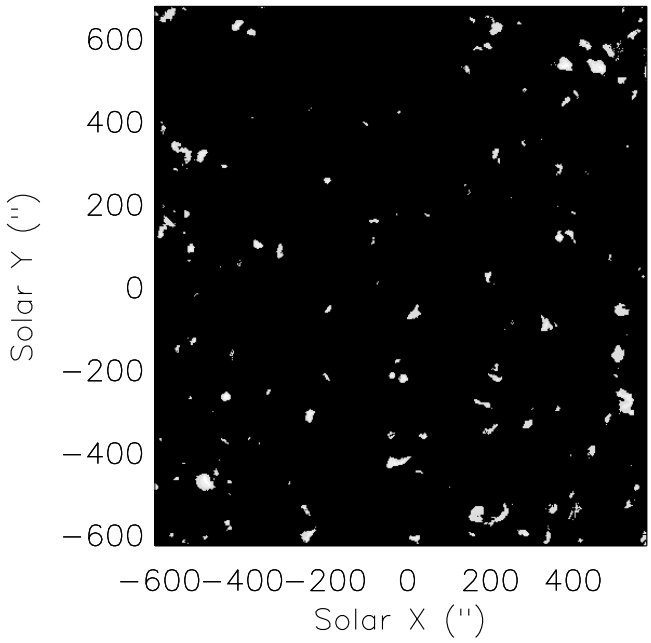

FIG. 5*b*

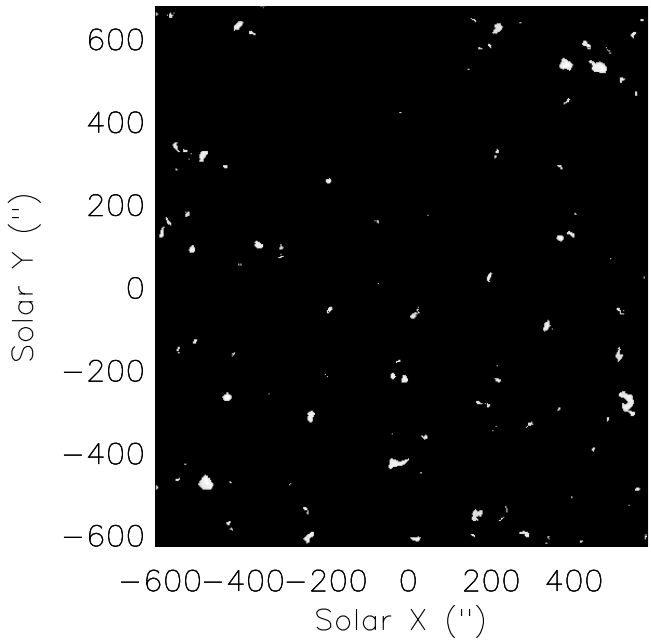

FIG. 5*c*

FIG. 5.—Part of an EIT image taken on 1996 November 6 (*panel a*); the same image, only with pixels brighter than 2 σ (*panel b*) and only with pixels brighter than 3 σ (*panel c*). [*See the electronic edition of the Journal for a color version of this figure.*]

of one full image (*panel a*) and after selection using the first criterion (*panel b*) or the second one (*panel c*). The processed images show only discrete structures from the emission maxima, eliminating the fuzzy quiet-Sun background. With the two criteria, images display the same structures, which are defined by more pixels of lower intensities in the case of 2σ.

4. DISCUSSION

In this paper we have performed two types of analysis on a data set obtained with the EIT instrument on board of *SOHO*. First, we have seen that the single-pixel histogram of intensities shows a departure from Gaussianity at large intensities. Associating the single pixel with the numerical box used in the theoretical simulations of a forced system governed by the MHD equations, this result can be explained as a signature of the fact that the portion of the Sun corresponding to a given pixel is filled by a turbulent plasma. This is because a histogram of intensities of a collection of pixels in space at different times can be considered statistically equivalent to a histogram of intensities of a single pixel followed in time. Therefore the tails in the observational and theoretical histograms have the same origin: the intermittent character of the nonlinear plasma dynamics, which transport energy from the injection scale to the dissipative scale. This dynamic owes its existence to the combined effect of stress induced by photospheric motions and new emerging flux on the coronal magnetic field, and may be described, theoretically, also in terms of interaction of wave motions, as long as one allows for the nonlinear character of such interactions. Phase mixing, resonance absorption, and other mechanisms invoking some kind of coherence or linearity of wave modes alone cannot, however, give rise to the signatures we have just discussed. They may indeed be present and occur, locally enhancing, even triggering, nonlinear dynamics, but they cannot be *the mechanism* of coronal heating. Historically, there has also been a distinction between the Parker nanoflare scenario and turbulent heating models; as mentioned in the introduction, the nanoflare scenario in fact may be considered as an average description of a magnetically dominated turbulent state.

Second, we have shown that outside large bright points observed on the quiet Sun, there remain observable brightenings in neighboring pixels of an image, which according to our interpretation are significantly correlated. Therefore they must be considered as single multipixel "events" over which the emission is integrated. The resulting histogram in terms of events displays a well-defined power law, which extends from many, low-intensity, single-pixel brightenings to fewer, brighter (with many pixels contributing), events. We have adopted two different definitions of "brightness," both based on the existence of a threshold between a low-energy Gaussian core in the single-pixel histogram and a high-intensity tail. The low-intensity part of the distribution, which is found also in the statistical analysis of theoretical time series, is in our opinion due to a *lack of resolution* both in theoretical studies and in observational data; by this we mean that pixel dimensions (or grid size in the simulations) are much larger than the real individual dissipative structure; in the simulations the Reynolds number is much smaller than real values, so some background dissipation occurs also outside the "singular" structures, which would be the only dissipative structures were the Reynolds number allowed to grow large; in the observations, besides other instrumental effects, there is in any case a line-of-sight smoothing that cannot be avoided. However, it is interesting to note that the resulting power laws do not seem to depend much on the choice of the criterion adopted to get rid of the noise.

Since the images used for our statistics were snapshots widely separated in time, we could not derive an overall emitted power from the intensity, which might seem a serious drawback in our study. As mentioned in § 1, different researchers have found power laws for the number of "events" associated with brightenings in the EIT emission lines of He II (transition region) and Fe XII. In any case, the total energy flux in observed EUV events is orders of magnitude lower than that required to sustain the corona, independently of the methods used to define an individual event (this conclusion was indeed reached by Habbal 1992 on the basis of a much wider survey of *Skylab* observations). The values of the energy power-law indices obtained are therefore of interest only in the way they affect subresolution energy extrapolations, with flatter power laws requiring a smaller minimum value for dissipative events, as long as $\alpha \leq -2$. However, straight-line extrapolations may well be invalid, as already shown in the variations between statistics in X-rays and EUV. Besides, it is even methodologically dubious to carry out extrapolations concerning a given phenomenon from observations of an energetically insignificant portion of the phenomenon itself. The strong result is the one concerning self-similarity, which cannot be considered as a random occurrence.

In this paper we have carried out a statistical analysis of the spatial characteristics in the Fe XII emission line of quiet-Sun regions. This analysis complements those of Berghmans et al. (1998) and Krucker & Benz (1998) in presenting evidence in favor of a turbulent mechanism of coronal energy release, with individual dissipative structures far below instrumental resolution. We have also discussed some of the questions involved in comparing observational data to numerical simulations of MHD turbulent processes. In particular, we plan to analyze numerical simulation results once again by taking a definition of events akin to the spatial events given here.

An interesting point will be to ensure that our conclusion in the variation of the power-law index is correct by using *TRACE* data that have a better resolution than EIT data. Its high spatial resolution will allow us to take into account smaller events, in size and in intensity.

G. Einaudi, M. Velli, and J. C. Vial would like to thank ISSI for the useful discussions and great atmosphere provided during its meetings. The authors thank the referee for his useful comments. V. Aletti thanks PNST (Programme National Soleil, Terre) and MURST (Ministero dell'Universita' et dela Ricerca Scientifica & Tecnologica) for financial support.

REFERENCES

Berghmans, D., Clette, F., & Moses, D. 1998, A&A, 336, 1039
Crosby, N., Aschwanden, M. J., & Dennis, B. R. 1993, Sol. Phys., 143, 275
Delaboudinière, J. P., et al. 1995, Sol. Phys., 162, 291
Dmitruk, P., Gomez, D. O., & DeLuca, E. E. 1998, ApJ, 505, 974
Einaudi, G., & Velli, M. 1999, Phys. Plasmas, 6, 4146
Einaudi, G., Velli, M., Politano, H., & Pouquet, A. 1996, ApJ, 457, L113
Georgoulis, M., Velli, M., & Einaudi, G. 1998, ApJ, 497, 957
Habbal, S. R. 1992, Ann. Geophys., 10, 34
Harrison, R. A. 1997, Sol. Phys., 175, 467
Hudson, H. S. 1991, Sol. Phys., 133, 357
Krucker, S., & Benz, A. O. 1998, ApJ, 501, L213 (KB)
Lin, R. P., Schwartz, R. A., Kane, S. R., Pelling, R. M., & Hurley, C. C. 1984, ApJ, 283, 421
Parker, E. N. 1988, ApJ, 330, 474
Ramaty, R., Mandzhavidze, N., Kozlovsky, B., & Murphy, R. J. 1995, ApJ, 455, L193
Schrijver, C. J., Title, A. J., & Van Ballejooijen, A. A. 1997, ApJ, 487, 424
Withbroe, L., & Noyes, R. W. 1977, ARA&A, 15, 363
Wu, S. T., et al. 1986, in Energetic Phenomena on the Sun, ed. M. Kundu & B. Woodgate (NASA CP-2439), 5